Inorg. Chem. **2005**, *44*, 6983–6988

Cyano-Bridged Hexanuclear Fe_4M_2 (M = Ni, Co, Mn) Clusters: Spin-Canted Antiferromagnetic Ordering of Fe_4Ni_2 Cluster

Jinkwon Kim,*,† Sujin Han,† Konstantin I. Pokhodnya,‡ Jesse M. Migliori,‡ and Joel S. Miller*,‡

Departments of Chemistry, Kongju National University, 182 Shinkwan, Chungnam 314-701, Korea, and University of Utah, 315 S. 1400 E. RM 2124, Salt Lake City, Utah 84112-0850

Received January 11, 2005

Heterobimetallic hexanuclear cyano-bridged complexes, $[\{Fe(Tp)(CN)_3\}_4\{M(MeCN)(H_2O)_2\}_2]\cdot 10H_2O\cdot 2MeCN$ [M = Ni (**1**), Co (**2**), Mn (**3**); Tp = hydrotris(1-pyrazolyl)borate], have been synthesized in H_2O–MeCN solution. Complexes **1**–**3** are isostructural and hexanuclear with $[\{Fe(Tp)(CN)_3\}_4\{M(MeCN)(H_2O)_2\}_2]$ units linked by hydrogen bonds to form a 2D-structure in the solid state. Complex **1** is a canted antiferromagnet that undergoes a field-induced spin-flop-like transition at ~1 T and 2 K. At 4.45 K **1** has a transition to paramagnetic state of noninteracting $S = 4$ magnetic clusters. However, **2** and **3** show antiferromagnetic intracluster coupling. Facile loss of solvent from **2** alters the local symmetry resulting in changing the intracluster interaction from antiferro- to ferromagnetic.

Introduction

The design and construction of coordination polymer materials exhibiting a spontaneous magnetization below critical temperature is an active area of contemporary research.[1] A variety of new molecule-based magnets have been synthesized by using first-row hexacyanides.[2−6] Reactions of $[M(CN)_6]^{q-}$ ($q = 3, 4$) and M'^{p+} ($p = 2, 3$) provide Prussian blue-structured heterobimetallic hexacyanometalates, some of which show magnetic ordering temperatures (T_c) higher than room temperature. In addition, interesting electrochemical and optomagnetic properties have been observed.[7,8] To understand the correlation between the crystal structure and the magnetism, various cyano-bridged materials of different dimensionalities have been extensively investigated.[9]

Another synthetic challenge in the field of molecule-based magnetism is to create superparamagnetic low-dimensional complexes which have high-spin ground states and large anisotropy and show very slow relaxation of their magnetization, i.e., so-called single-molecule magnets (SMMs)[10] and single-chain magnets (SCMs).[11] Various cyano-bridged poly-

* To whom correspondence should be addressed. E-mail: jkim@kongju.ac.kr (J.K.); jsmiller@chem.utah.edu (J.S.M.).
† Kongju National University.
‡ University of Utah.

(1) Reviews: (a) Ovcharenko, V. I.; Sagdeev, R. Z. *Russ. Chem. Rev.* **1999**, *68*, 345. (b) Kinoshita, M. *Philos. Trans. R. Soc. London A* **1999**, *357*, 2855. (c) Miller, J. S.; Epstein, A. J. *Chem. Commun.* **1998**, 1319. (d) Day, P. *J. Chem. Soc., Dalton Trans.* **1997**, 701. (e) Miller, J. S.; Epstein, A. J. *Chem. Eng. News* **1995**, *73*, 3 (40), 30. (f) Miller, J. S.; Epstein, A. J. *Adv. Chem. Ser.* **1995**, *245*, 161. (g) Miller, J. S.; Epstein, A. J. *Angew. Chem., Int. Ed. Engl.* **1994**, *33*, 385. (h) Kahn, O. *Adv. Inorg. Chem.* **1995**, *43*, 179. (i) Gatteschi, D. *Adv. Mater.* **1994**, *6*, 635. (j) Kahn, O. *Molecular Magnetism*; VCH Publishers: New York, 1993. (k) Crayson, J. A.; Devine, J. N.; Walton, J. C. *Tetrahedron* **2000**, *56*, 7829. Blundell, S. J.; Pratt, F. L. *J. Phys.: Condens. Matter* **2004**, *16*, R771.
(2) Verdaguer, M.; Bleuzen, A.; Marvaud, V.; Vaissermann, J.; Seuleiman, M.; Desplanches, C.; Scuiller, A.; Train, C.; Garde, R.; Gelly, G.; Lomenech, C.; Rosenman, I.; Veillet, P.; Cartier, C.; Villain, F. *Coord. Chem. Rev.* **1999**, *190−192*, 1023.
(3) Mallah, T.; Thiébaut, S.; Verdaguer, M.; Veillet, P. *Science* **1993**, *262*, 1544.
(4) Ferlay, S.; Mallah, T.; Ouahès, R.; Veillet, P.; Verdaguer, M. *Nature* **1995**, *378*, 701.
(5) (a) Entley, R. W.; Girolami, G. S. *Inorg. Chem.* **1994**, *33*, 5165 (b) Entley, R. W.; Girolami, G. S. *Science* **1995**, *268*, 397. (c) Holmes, S. M.; Girolami, G. *J. Am. Chem. Soc.* **1999**, *121*, 5593.
(6) (a) Halevik, Ø.; Buschmann, W. E.; Zhang, J.; Manson, J.; Miller, J. S. *Adv. Mater.* **1999**, *11*, 914. (b) Buschmann, W. E.; Paulson, S. C.; Wynn, C. M.; Girtu, M.; Epstein, A. J.; White, H. S.; Miller, J. S. *Adv. Mater.* **1997**, *9*, 645. (c) Buschmann, W. E.; Paulson, S. C.; Wynn, C. M.; Girtu, M.; Epstein, A. J.; White, H. S.; Miller, J. S. *Chem. Mater.* **1998**, *10*, 1386.
(7) (a) Sato, O.; Iyoda, T.; Fujishima, A.; Hashimoto, K. *Science* **1996**, *271*, 49. (b) Ohkoshi, S.-I.; Fujishima, A.; Hashimoto, K. *J. Am. Chem. Soc.* **1998**, *120*, 5349. (c) Mizno, M,; Ohkoshi, S.-I.; Hashimoto, K. *Adv. Mater.* **2000**, *12*, 1955.
(8) (a) Sato, O.; Iyoda, T.; Fujishima, A.; Hashimoto, K. *Science* **1996**, *271*, 704. (b) Sato, O.; Einaga, T.; Fujishima, A.; Hashimoto, K. *Inorg. Chem.* **1999**, *38*, 4405.
(9) Ohba, M.; Okawa, H. *Coord. Chem. Rev.* **2000**, *198*, 313.
(10) Gatteschi, D.; Sessoli, R. *Angew. Chem., Int. Ed.* **2003**, *42*, 268.
(11) (a) Caneschi, A.; Gatteschi, D.; Lalioti, N.; Sangregorio, C.; Sessoli, R.; Veturi, G.; Vindigni, A.; Rettori, A.; Pini, M. G.; Novak, M. A. *Angew. Chem., Int. Ed.* **2001**, *40*, 1760. (b) Clérac, R.; Miyasaka, H.; Yamashita, M.; Coulton, C. *J. Am. Chem. Soc.* **2002**, *124*, 12837. (a) Pardo, E.; Ruíz-Garcia, R.; Lloret, F.; Faus, J.; Julve, M.; Journaux, Y.; Delgado, F.; Ruiz-Pérez, C. *Adv. Mater.* **2004**, *16*, 1597. (d) Miyasaka, H.; Nezu, T.; Sugimoto, K.; Sugiura, K.; Yamashita, M.; Clérac, R. *Chem.*—Eur. J. **2005**, *11*, 1592.

10.1021/ic0500356 CCC: $30.25
Published on Web 09/01/2005

nuclear complexes have been prepared by using molecule-based building blocks such as $[M(CN)_6]^{3-}$ (M = Cr, Fe), $[Mo(CN)_8]^{3-}$, *fac*-$[M(L_3)(CN)_3]$ (M = Cr, Fe, Co, Mo), $[Fe(L)_2(CN)_4]^-$, and $[Fe(L)_4(CN)_2]^-$.[12−18] An $Mn^{II}_9Mo^{V}_6$ tridecacyano cluster has an $S = 39/2$ ground-state spin, but it does not exhibit hysteresis, related to a slow relaxation of the magnetization.[13b] In contrast, trigonal prismatic $[(Me_3tacn)_2MnCr_6(CN)_{18}]^{2+}$ (Me_3tacn = 1,4,7-trimethyltriazacyclononane) shows frequency dependence in out-of-phase ac susceptibility.[14c] The one-dimensional cyano-bridged heterobimetallic chains $\{[Ni(rac\text{-}CTH)]_3[Fe(CN)_6]_4\}_n$ (*rac*-CHT = 5,7,7,12,14,14-hexamethyl-1,4,8,11-tetraazacyclotetradecane),[15a] $(NEt_4)[Mn_2(5\text{-}MeOsalen)_2Fe(CN)_6]$ ($MeOsamlen^{2-}$ = *N*,*N*′-ethylenebis(5-methoxysalicylideneiminate),[15c] and $[(Tp)_2Fe_2(CN)_6Cu(CH_3OH)\cdot 2CH_3OH]_n$[16b] are the examples exhibiting slow relaxation of magnetization. To expand the molecular chemistry for magnetic materials, we recently utilized a new building block, [*fac*-Fe(Tp)$(CN)_3]^-$ [Tp = hydrotris(1-pyrazolyl)borate],[19,20] and synthesized heteronuclear cyano-bridged complexes $[MnFe_2(Tp)_2(CN)_6(CH_3OH)_4]$ and $[Mn_2Fe_2(Tp)_2(CN)_6(4,4'\text{-bipyridine})_2](ClO_4)_2$,[20] and we herein report hexanuclear cyano-bridged $[\{(Tp)Fe(CN)_3\}_4\{M(MeCN)(H_2O)_2\}_2]\cdot 10H_2O\cdot 2MeCN$ [M = Ni (**1**), Co (**2**), Mn (**3**)], of which the **1** shows a ferromagnetic phase transition below 4 K.

Experimental Section

Methods and Materials. All reactions were performed under aerobic conditions. Solvents (MeCN, Et_2O) and reagents (Tp, $Ni(NO_3)_2\cdot 6H_2O$, $Co(ClO_4)_2\cdot 6H_2O$, $Mn(ClO_4)_2\cdot 6H_2O$) were purchased from Aldrich chemical Co. and used as received. (Et_4N)[*fac*-Fe(Tp)$(CN)_3$] was prepared as described.[20]

$[\{Fe(Tp)(CN)_3\}_4\{Ni(MeCN)(H_2O)_2\}_2]\cdot 10H_2O\cdot 2MeCN$ (1). A solution of 29 mg (0.1 mmol) of $Ni(NO_3)_2\cdot 6H_2O$ in 10 mL of water was allowed to react with slowly a solution of 96 mg (0.2 mmol) of (Et_4N)[*fac*-Fe(Tp)$(CN)_3$] in 10 mL of MeCN at room temperature. Brownish red solids were precipitated immediately and were not dissolved in most organic solvents. To obtain larger crystals, two solutions were reacted very slowly using a syringe pump. The resulting red crystals were collected by filtration and washed with water, MeCN, and diethyl ether to remove unreacted chemicals. Yield: 64 mg (33%). FTIR (KBr, cm^{-1}): ν(BH) = 2517 (m), ν(CN) = 2162 (s), 2128 (m). Anal. Calcd for $C_{56}H_{80}B_4Fe_4N_{40}Ni_2O_{14}$: C, 35.00; H, 4.20; N, 29.16. Found: C, 34.68; H, 4.27; N, 28.98.

$[\{Fe(Tp)(CN)_3\}_4\{Co(MeCN)(H_2O)_2\}_2]\cdot 10H_2O\cdot 2MeCN$ (2). A solution of 37 mg (0.1 mmol) of $Co(ClO_4)_2\cdot 6H_2O$ in 10 mL of water was added slowly to a flask containing 96 mg (0.2 mmol) of (Et_4N)[*fac*-Fe(Tp)$(CN)_3$] in 10 mL of MeCN at room temperature via syringe pump. The resulting red crystals were collected by filtration and washed with water, MeCN, and diethyl ether. Yield: 70 mg (36%). FTIR (KBr, cm^{-1}): ν(BH) = 2514 (m), ν(CN) = 2158 (s), 2128 (m). Anal. Calcd for $C_{56}H_{80}B_4Co_2Fe_4N_{40}O_{14}$: C, 34.99; H, 4.19; N, 29.15. Found: C, 34.72; H, 4.21; N, 28.63.

$[\{Fe(Tp)(CN)_3\}_4\{Mn(MeCN)(H_2O)_2\}_2]\cdot 10H_2O\cdot 2MeCN$ (3). A solution of 36 mg (0.1 mmol) of $Mn(ClO_4)_2\cdot 6H_2O$ in 10 mL of water was added slowly to a flask containing 96 mg (0.2 mmol) of (Et_4N)[*fac*-Fe(Tp)$(CN)_3$] in 10 mL of MeCN at room temperature via syringe pump. The resulting red crystals were collected by filtration and washed with water, MeCN, and diethyl ether. Yield: 85 mg (44%). FTIR (KBr, cm^{-1}): ν(BH) = 2515 (m), ν(CN) = 2151 (s), 2127 (m). Anal. Calcd for $C_{56}H_{80}B_4Co_2Fe_4N_{40}O_{14}$: C, 35.14; H, 4.21; N, 29.27. Found: C, 35.08; H, 4.03; N, 28.76.

X-ray Crystallography. Single crystals suitable for X-ray crystallography were grown by slow diffusion of solution of M^{II} in water and (Et_4N)[*fac*-Fe(Tp)$(CN)_3$] in MeCN. Red single crystals of compounds **1** and **2** were coated with Parathone-N oil and mounted on a glass fiber. The crystals were then placed on a Bruker AXS SMART diffractometer equipped with a CCD detector in a nitrogen cold stream maintained at 150 K. More than a hemisphere of data was collected on each crystal over three batches of exposure using Mo Kα radiation (λ = 0.710 73 Å). A fourth set of data was measured and compared to the initial set to monitor and correct for decay, which was negligible in all cases. Data processing was then performed using the program SAINT.[21] A red single crystal of **3** was sealed in a glass tube and mounted on an Enraf-Nonius CAD4 diffractometer with graphite-monochromated Mo Kα radiation (λ = 0.710 73 Å). The structures of the compounds were solved by the direct methods and refined by the full-matrix least-squares method on all F^2 data using SHELX 97.[22] The anisotropic thermal parameters for all non-hydrogen atoms were included in the refinements. All hydrogen atoms bonded to carbon atoms were included in calculated positions. The C−H bond distances were fixed, and the *U* values were assigned approximately on the basis of the *U* value of the attached atom. The crystal and refinement data are summarized in Table 1.

Thermal Properties. The thermal properties were studied using a TA Instruments model 2050 thermogravimetric analyzer (TGA) equipped with a TA-MS Fison triple-filter quadrupole mass

(12) (a) Scillier, A.; Mallah, T.; Verdaguer, M.; Nivorozkhin, A.; Tholence, J. L.; Veillet, P. *New J. Chem.* **1996**, *20*, 1. (b) Vostrikova, K. E.; Luneau, D.; Wersdorfer, W.; Rey, P.; Verdaguer, M. *J. Am. Chem. Soc.* **2000**, *122*, 718. (c) Rogez, G.; Marvilliers, A.; Rivière, E.; Audière, J.-P.; Lloret, F.; Varret, F.; Goujon, A.; Mendenez, N.; Girerd, J.-J.; Mallah, T. *Angew. Chem., Int. Ed.* **2000**, *39*, 2885.

(13) (a) Larionova, J.; Gross, M.; Pilkingto, M.; Andres, H.; Stoeckli-Evans, H.; Güdel, H. U.; Decurtins, S. *Angew. Chem., Int. Ed.* **2000**, *39*, 1605. (b) Ruiz, E.; Rajaraman, G.; Alvarez, S.; Gillon, B.; Stride, J.; Clérac, R.; Larionova, J.; Decurtins S. *Angew. Chem., Int. Ed.* **2005**, *44*, 2711. (c) Zhong, Z. J.; Seino, H.; Mizobe, Y.; Hidai, M.; Fujishima, A.; Ohkoshi, S.-I.; Hashimoto, K. *J. Am. Chem. Soc.* **2000**, *122*, 2952.

(14) (a) Heinrich, J. L.; Berseth, P. A.; Long, J. *Chem. Commun.* **1998**, 1231. (b) Sokol, J. J.; Shores, M. P.; Long, J. R. *Inorg. Chem.* **2002**, *41*, 3052. (c) Sokol, J. J.; Hee, A. G.; Long, J. R. *J. Am. Chem. Soc.*, **2002**, *124*, 7655. (d) Yang, J. Y.; Shores, M. P.; Sokol, J. J.; Long, J. R. *Inorg. Chem.* **2003**, *42*, 1403.

(15) (a) Colacio, E.; Domínguez-Vera, J. M.; Lloret, F.; Rodriquez, A.; Stoeckli-Evans, H. *Inorg. Chem.* **2003**, *42*, 6962. (b) Choi, H. J.; Sokol, J. J.; Long, J. *Inorg. Chem.* **2004**, *43*, 1606. (c) Ferbinteanu, M.; Miyasaka, H.; Werensdofer, W.; Nakata, K.; Sugiura, K.; Yamashita, M.; Coulton, C.; Clérac, R. *J. Am. Chem. Soc.* **2005**, *127*, 3090.

(16) (a) Lescouëzec, R.; Vaissermann, J.; Toma, L. M.; Carrasco, R.; Lloret, F.; Julve, M. *Inorg. Chem.* **2004**, *43*, 2234. (b) Wang S.; Zuo, J.-L.; Gao, S.; Song, Y.; Zhou, H.-C.; Zhang, Y.-Z.; You, X.-Z. *J. Am. Chem. Soc.* **2004**, *126*, 8900.

(17) (a) Lescouëzec, R.; Lloret, F.; Julve, M.; Vaissermann, J.; Verdaguer, M.; Llusar, R.; Uriel, S. *Inorg. Chem.* **2001**, *40*, 2065. (b) Lescouëzec, R.; Lloret, F.; Julve, M.; Vaissermann, J.; Verdaguer, M.; Llusar, R. *Inorg. Chem.* **2002**, *41*, 818.

(18) (a) Oshio, H.; Tamada, O.; Onodera, H.; Ito, T.; Ikoma, T.; Tero-Kubota, S. *Inorg. Chem.* **1999**, *38*, 5686. (b) Oshio, H.; Onodera, H.; Tamada, O.; Mizutani, H.; Hikichi, T.; Ito, T. *Chem.*—Eur. J. **2000**, *6*, 2523. (c) Ni, Z.-H.; Kou, H.-Z.; Zhao, Y.-H.; Zheng, L.; Wang, R.-J.; Cui, A.-L.; Sato, O. *Inorg. Chem.* **2005**, *44*, 2050.

(19) Lescouëzec, R.; Vaissermann, J.; Lioret, F.; Julve, M.; Verdaguer, M. *Inorg. Chem.* **2002**, *115*, 13976.

(20) Kim, J.; Han, S.; Cho, I.-K.; Choi, K. Y.; Heu, M.; Yoon, S.; Suh, B.-J. *Polyhedron* **2004**, *23*, 1333.

(21) SA*INT-Plus*, version 6.02; Bruker Analytical X-ray System: Madison, WI, 1999.

(22) Sheldrick, G. M. *SHELX 97*; Universität of Göttingen: Göttingen, Germany, 1997.

Table 1. Details of the Crystallographic Data Collection for **1**−**3**

param	**1**	**2**	**3**
chem formula	$C_{56}H_{80}B_4Fe_4N_{40}Ni_2O_{14}$	$C_{56}H_{80}B_4Co_2Fe_4N_{40}O_{14}$	$C_{56}H_{80}B_4Fe_4Mn_2N_{40}O_{14}$
fw	1921.66	1922.10	1914.12
space group	$P2_1/c$	$P2_1/c$	$P2_1/c$
a/Å	13.485(6)	13.512(1)	13.594(2)
b/Å	14.332(6)	14.356(1)	14.505(3)
c/Å	21.954(9)	22.119(1)	22.493(4)
β/deg	106.22(1)	105.80(1)	105.49(2)
V/Å^3	4074(3)	4128.6(5)	4274(1)
Z	2	2	2
ρ(calcd)/g cm^{-3}	1.566	1.546	1.487
μ/mm^{-1}	1.230	1.160	1.028
no. of unique reflcns	9418	7474	7507
reflcns with $I > 2\sigma(I)$	6714	4769	6061
2q max/°	50	56	56
no. of params refined	533	543	543
R(F), wR(F^2)	0.1318, 0.2320	0.0438, 0.1003	0.0535, 0.1413
GOF	1.206	0.919	1.052

Table 2. Selected Bond Lengths (Å) and Bond Angles (deg) for Complex **1**−**3**

param	**1**	**2**	**3**
Fe1···M	5.016(2)	5.0729(8)	5.154(1)
Fe2···M	5.126(2)	5.1758(7)	5.258(1)
Fe1−C10	1.93(1)	1.929(4)	1.924(4)
Fe1−C11	1.92(1)	1.919(4)	1.918(4)
Fe1−C12	1.92(1)	1.939(4)	1.922(4)
M−N7	2.045(8)	2.108(4)	2.200(3)
M−N16	2.062(8)	2.108(3)	2.205(3)
M−N17[a]	2.084(8)	2.127(4)	2.222(4)
M−N19	2.107(8)	2.161(3)	2.285(4)
M−O1	2.049(7)	2.059(3)	2.159(3)
M−O2	2.076(6)	2.084(3)	2.198(3)
N7−M−N16	96.2(3)	97.0(1)	96.9(1)
N7−M−N19	83.4(3)	83.1(1)	83.2(1)
N7−M−O1	89.0(3)	90.0(1)	90.0(1)
N7−M−O2	90.0(3)	90.3(1)	90.6(1)
N16−M−N19	176.8(3)	176.2(1)	174.9(2)
N16−M−N17[a]	91.9(3)	91.3(1)	92.6(1)
N16−M−O1	91.5(3)	91.7(1)	91.5(1)
N16−M−O2	88.0(3)	87.6(1)	87.0(1)
N19−M−N17[a]	88.3(3)	88.4(1)	87.0(2)
N19−M−O1	91.7(3)	92.1(1)	93.6(2)
N19−M−O2	88.8(3)	88.6(1)	87.9(2)
O1−M−O2	178.9(3)	179.3(1)	178.4(1)

[a] Symmetry transformations used to generate equivalent atoms: $-x+1, -y+2, -z+1$.

spectrometer to identify gaseous products with masses less than 300 amu. It is located in a DriLab glovebox that uses N_2 to protect air- and moisture-sensitive samples. Samples were placed in an aluminum pan and heated at 5 °C/min under a continuous 10 mL/min nitrogen flow.

Magnetic Measurements. The magnetic susceptibility, χ, was determined either on a Quantum Design 5 T MPMS magnetometer or 9 T PPMS susceptometer as previously described.[23] To minimize solvent loss, all samples were loaded while the MPMS at 150 K. The diamagnetic corrections, which were calculated from the Pascal constants, are 926 × 10^{-6}, 930 × 10^{-6}, and 934 × 10^{-6} emu/mol for **1**−**3**, respectively.

Results and Discussions

Compounds **1**−**3** were synthesized by the reaction of [*fac*-Fe(Tp)(CN)$_3$]$^-$ in MeCN and M^{II} (M = Ni, Co, Mn) in H_2O. The structure of the neutral Fe_4M_2 hexanuclear unit has two [Fe(Tp)(CN)$_3$]$^-$ anions which act as bidentate ligands to bridge M^{II} ions through cyanide groups forming an [Fe_2M_2(CN)$_4$]$^{6+}$ square unit (Figure 1). Two [Fe(Tp)(CN)$_3$]$^-$ anions are bound to two M^{II} ions with cis−trans geometry with respect to the bridging [Fe(Tp)(CN)$_3$]$^-$ anion. The [Fe_4M_2(CN)$_6$]$^{10+}$ unit is approximately coplanar (average value of rms deviation is 0.316 Å for **1**). The average intramolecular Fe···Ni, Fe···Co, and Fe···Mn distances are 5.071, 5.124, and 5.206 Å, respectively (Table 2). Each M^{II} is coordinated by two water and one acetonitrile molecules. Ten unbound H_2O and two MeCN molecules exist between cyano-bridged Fe_4M_2 clusters. The Fe_4M_2 molecules are linked through hydrogen bonds (Table 3) involving coordinated and uncoordinated water molecules and nitrogen atoms of terminal CN groups (Figure 2). The O···O distances are in the range 2.720(6)−3.092(6) Å, and N···O distances , in the range 2.772(5)−3.020(6) Å (Table 3).

Crystals of **1** were too small to complete structure solving with a high degree of accuracy (R = 0.13). Nevertheless, the unit cell parameters of **1** and other spectroscopic data are quite similar to those of **2** and **3** (Table 1); i.e., **1** is isomorphous to **2** and **3**.

The 5−300 K temperature dependence of the magnetic susceptibility, χ, of **1** is reported as $\chi T(T)$ and $\chi^{-1}(T)$ [$\propto(T-\Theta)$], Figure 3. The $\chi T(T)$ is nearly temperature independent above 100 K and at 300 K has values of 5.4 emu K/mol. This is in the range expected for four noninteracting

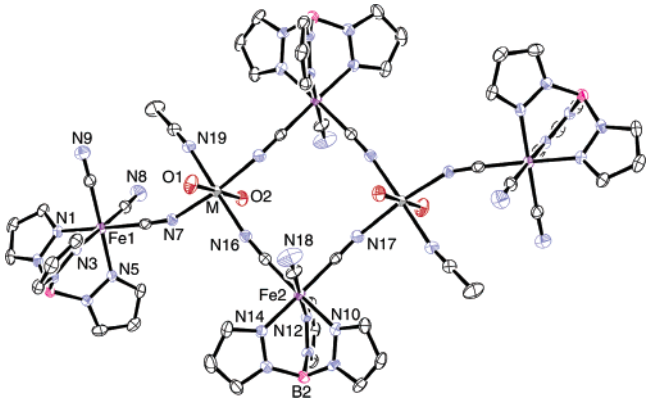

Figure 1. ORTEP (50%) diagram of [{Fe(Tp)(CN)$_3$}$_4${M(MeCN)(H$_2$O)$_2$}$_2$] (M = Mn, Co, Ni).

(23) Brandon, E. J.; Rittenberg, D. K.; Arif, A. M.; Miller, J. S. *Inorg. Chem.* **1998**, *37*, 3376.

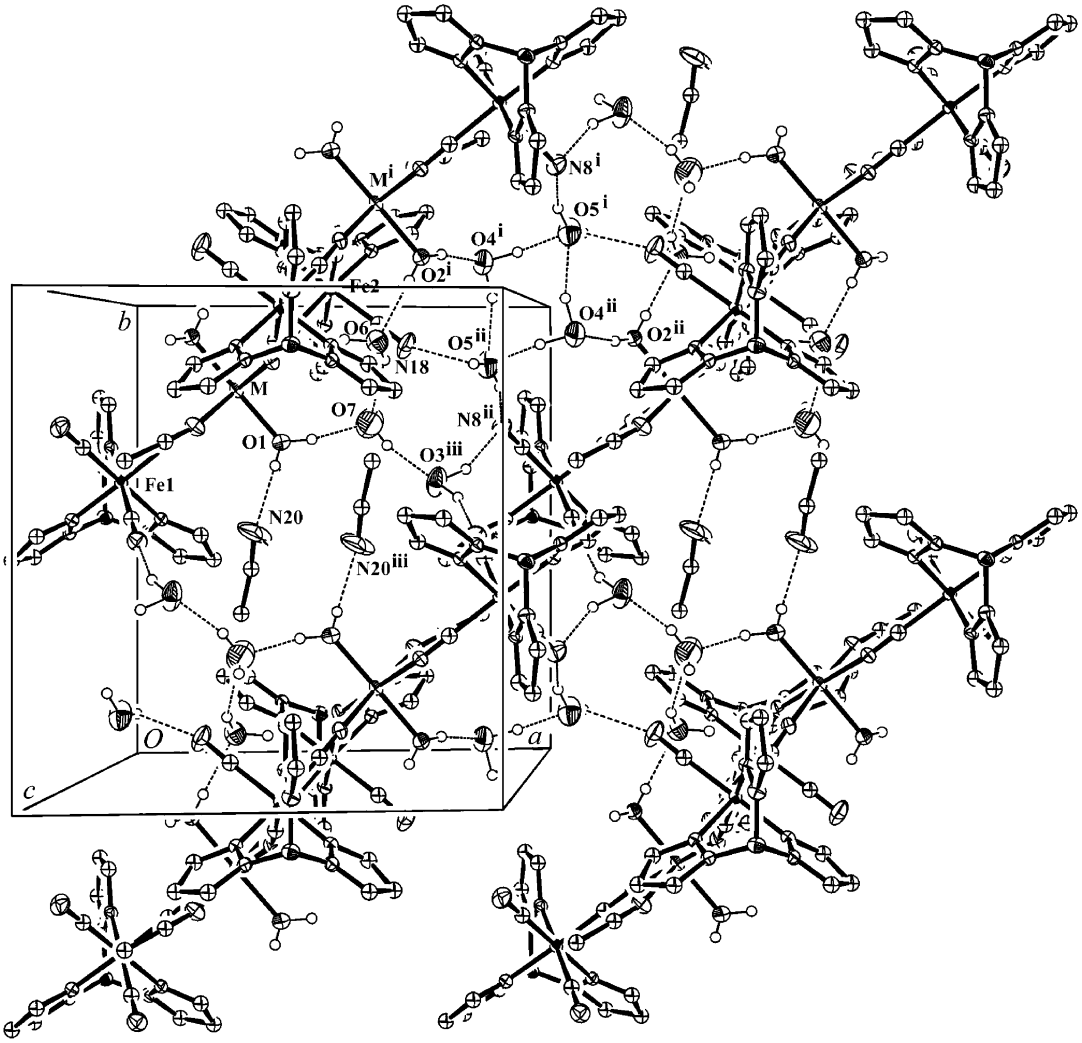

Figure 2. Crystal packing diagram of $[\{Fe(Tp)(CN)_3\}_4\{M(MeCN)(H_2O)_2\}_2]\cdot 10H_2O\cdot 2MeCN$ to illustrate hydrogen bonds. Symbols ′, ″, and ‴ represent symmetry transformations used to generate equivalent atoms by $(-1 + x, 1 - y, -z)$, $(1 + x, y, z)$, and $(-x, 1 - y, -z)$, respectively.

Table 3. Hydrogen Bonds (Å) for Complex **2**[a]

O1···O7	2.766(6)	O1···N20	2.826(5)
O2···O4	2.793(4)	O2^{i}···O6	2.825(4)
O3^{iii}···O7	2.720(5)	O3^{iii}···N8^{ii}	3.020(5)
O4···O5	2.792(6)	O4^{i}···O5^{ii}	3.092(5)
O5···N8	2.772(5)	O5^{ii}···N18	2.833(6)
O6···O7	2.975(5)	O7···N18	2.903(6)

[a] Symmetry transformations used to generate equivalent atoms: (i) $1 - x, 2 - y, 1 - z$; (ii) $1 + x, y, z$; (iii) $1 - x, 1 - y, 1 - z$.

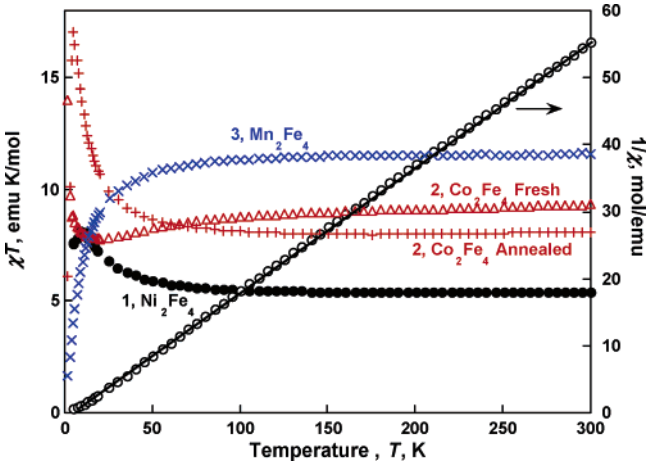

Figure 3. $\chi T(T)$ (●) and $\chi^{-1}(T)$ (○) for **1** with χT(300 K) = 5.4 emu K/mol and $\Theta = 3.1$ K (fitted by Curie−Weiss law, solid line) and $\chi T(T)$ for freshly filtered **2** (△) and **3** (×) and annealed **2** (+) with χT(300 K) of 8.9, 11.6, and 8.1 emu K/mol, respectively. Above 50 K **3** can be fit to the Curie−Weiss law with $\Theta = -3.7$ K, while $\Theta = -3.3$ for fresh **2** above 30 K. Annealed **2** can be fit with $\Theta = 3.6$ K between 20 and 1800 K.

octahedral $S = 1/2$ low-spin Fe^{III} ions, with $\chi T \sim 0.72$ emu K/mol,[24a] and two $S = 1$ high-spin Ni^{II}, with χT of ~1.3 emu K/mol.[24b]

Below 100 K, $\chi T(T)$ increases indicating that the metal ions of the $Ni^{II}_2Fe^{III}_4$ cluster unit couple ferromagnetically at low temperature. Above ~20 K $\chi^{-1}(T)$ can be fit to the Curie−Weiss expression with $\Theta = 3.1$ K. The positive Θ indicates ferromagnetic coupling, as expected for adjacently bonded low-spin Fe^{III} ($t_{2g}^5e_g^0$) and Ni^{II} have ($t_{2g}^6e_g^2$) that have their unpaired electron spins in orthogonal orbitals.[1h] Such ferromagnetic coupling has been observed for $Ni^{II}_3[Cr^{III}$-

(24) Casey, A. T.; Mitra, S. Magnetic Behavior of Compounds Containing d^n Ions. In *Theory and Applications of Molecular Paramagnetism, 1*; Boudreaux, E. A., Mulay, L. N., Eds.; John Wiley & Sons: New York, 1976. The reported range (a) for low-spin Fe^{III} is $0.56 \le \chi T \le 0.75$ (p 0.190), (b) for Ni^{II} is $0.97 \le \chi T \le 1.30$ (p 226), (c) for Co^{II} is $2.42 \le \chi T \le 3.40$ (p 214), and (d) for Mn^{II} is $3.25 \le \chi T \le 4.47$ (p 185).

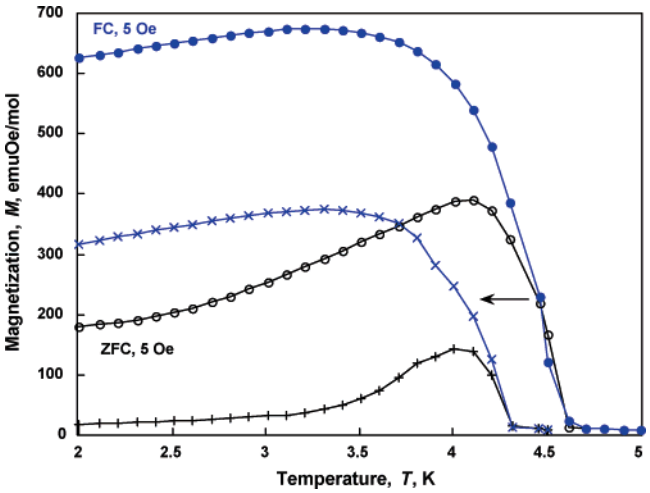

Figure 4. $M_{ZFC}(T)$ (○) and $M_{FC}(T)$ (●) for **1** in a 5 Oe external field. $M_{ZFC}(T)$ (+) and $M_{FC}(T)$ (×) of the same sample annealed in a vacuum at 300 K for 2 h.

$(CN)_6]_2 \cdot xH_2O$[25a] and $[Ni^{II}(tn)_6]_5[Fe^{III}(CN)_6](ClO_4) \cdot 2.5H_2O$ (tn = trimethylenediamine) with $T_c \sim 10$ K.[25b]

Below 20 K, $\chi T(T)$ increases rapidly with decreasing temperature reaching a maximum of 8.2 emu K/mol at $T_{max} \sim 10$ K and then decreases slightly (~4%) with temperature down to 5 K. Presumably, the decrease of $\chi T(T)$ below T_{max} indicates that intercluster antiferromagnetic coupling begins to compete with the ferromagnetic intracluster interactions.

The zero-field-cooled (ZFC) dc magnetization, $M_{ZFC}(T)$, increases abruptly below 4.6 K indicating a magnetic transition (Figure 4). The $M_{ZFC}(T)$ reaches rounded maximum at 4.1 K and then decreases gradually upon further cooling suggesting the antiferromagnetic ground state for **1**. The maximum in $M_{ZFC}(T)$ shifts to lower temperatures, and its amplitude decreases at higher applied magnetic fields as the easy axis spin alignment begins to compete with the internal AF ordering. Note that, in contrast to the $M_{ZFC}(T)$ behavior, the field-cooled (FC) magnetization $M_{FC}(T)$ only slightly decreases upon cooling to 2 K. The difference between $M_{ZFC}(T)$ and $M_{FC}(T)$ increases below a characteristic bifurcation temperature, $T_b \sim 4.5$ K, indicating the presence of a remanent magnetization below T_b, which increases upon cooling. Taking into account that the monoclinic unit cell of **1** consists of two independent magnetic clusters, we assume that their spins are not exactly antiparallel at low temperatures, and the ground state of **1** is a canted antiferromagnet.

The magnetic transition also reveals itself as a sharp narrow peak at 4.45 K in both the in-phase $\chi'(T)$ and the out-of phase $\chi''(T)$ components of the ac susceptibility (Figure 5). The peak positions in $\chi'(T)$ and $\chi''(T)$ are frequency (f) independent suggesting a good crystallinity; however, the feature (low-temperature side) absorption shifts toward higher temperatures with increasing frequency, which is typical for a highly disordered spin-glasses.[26]

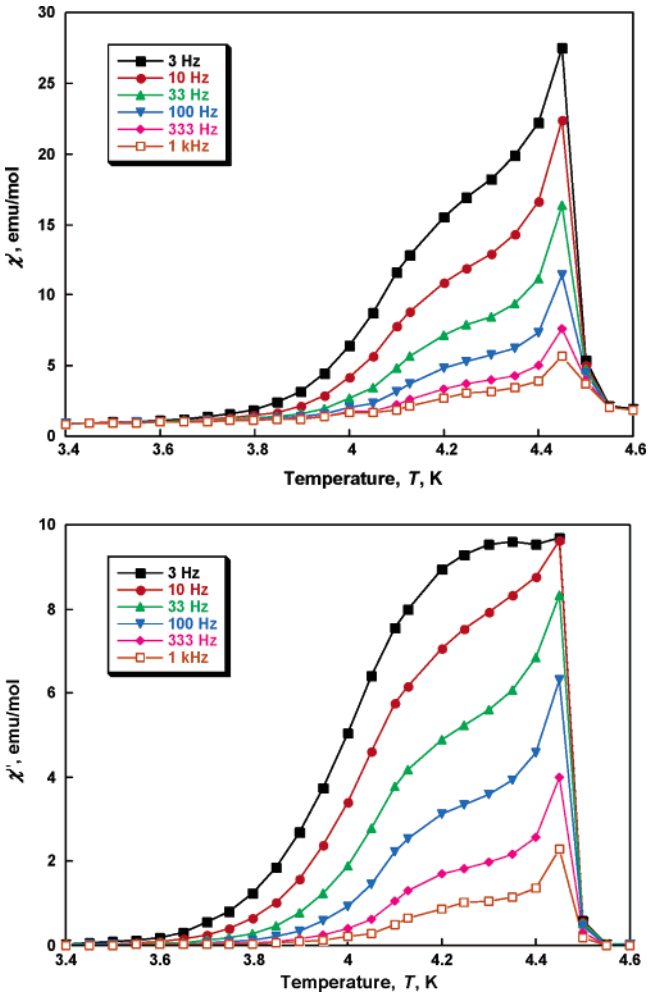

Figure 5. In-phase [$\chi'(T)$] and out-of phase [$\chi''(T)$] components of the ac susceptibility of **1** measured at frequencies $3 \leq 2\pi\omega \leq 1$ kHz in an applied ac field of 1 Oe.

The structure of **1** contains 2 MeCN and 10 H_2O solvent molecules that can be removed under relatively very mild conditions. A TGA study reveals that **2** starts to lose mass (up to ~8% during the first 1 h) in a dry N_2 flow even at ambient conditions. On warming, the mass spectrometer starts to register CH_3CN, and finally above 150 °C CN and C_2N_2 appear suggesting decomposition. It should be noted that **1** has a shift in T_c (~0.2 K) after being placed in a vacuum of 7 Torr at 300 K for 2 h (inside the magnetometer) (Figure 4). The inhomogeneous broadening of the $\chi'(T)$ peak, as well as T_c shift, can be attributed to partial solvent loss that created a structural disorder which suppresses the AF transition.

The field dependence of the magnetization, $M(H)$, reveals another magnetic transition (Figure 6). $M(H)$ for **1** rises rapidly with increasing field at low field and then slowly tends toward saturation at ~5600 emu Oe/mol in accord with it being a canted antiferromagnet. The hysteresis loop (Figure 6 inset) with coercive field, H_{cr}, of ~20 Oe suggests a substantial remanent magnetization (~700 emu Oe/mol) at 2 K. H_{cr} increases up to 100 Oe after being in vacuo at 300 K for 2 h; thus, the observed remanence is attributed to a frozen disorder associated with solvent vacancies.

(25) (a) Ohkoshi, S.; Iyoda,; Fujishima, A.; Hashimoto, K. *Phys. Rev.* **1997**, *56*, 11642. (b) Zhang, S.-W.; Fu, D.-G., Sun, W.-Y.; Hu, Z.; Yu, K.-B.; Tang, W.-X. *Inorg. Chem.* **2000**, *39*, 1142.
(26) Mydosh, J. A. *Spin Glasses*; Taylor & Francis: London, Washington, DC, 1993; p 67.

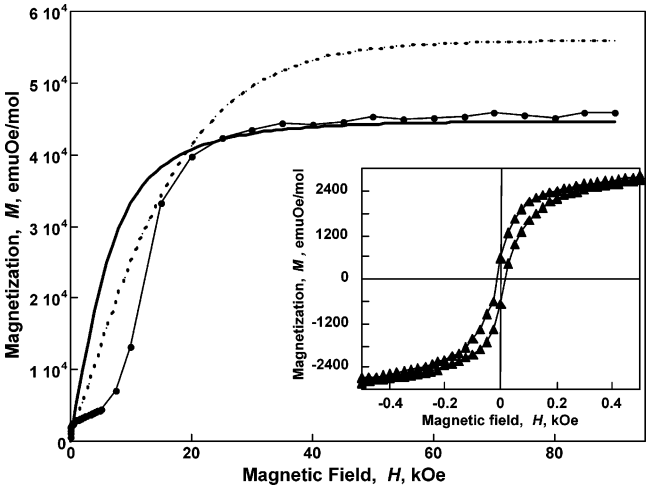

Figure 6. $M(H)$ for **1** (●) measured at 2 K using both SQUID and PPMS magnetometers. The dotted line is the magnetization calculated via the Brillouin function at 2 K as a sum of contributions from four $S = 1/2$ Fe^{III} ions and two $S = 1$ Ni^{II} ions; a solid line is the same for the cluster with $S = 4$ ($g = 2$). The inset displays the hysteresis loop measured at 2 K.

As the field increases above 5 kOe, $M(H)$ starts to rise again indicating a field induced spin-flop like transition. $M(H)$ saturates at ~45 000 emu Oe/mol consistent with an $S = 4$ cluster.[27] The random field associated with the highly disordered structure can suppress both the antiferromagnetic ordering and the field-induced transition. Note that at 5 K all these effects disappear and the $M(H)$ behaves in accord with those for the system of noninteracting $S = 4$ clusters.

The 2−300 K $\chi T(T)$ values of isostructural **2** and **3** are nearly temperature independent above ~150 K (Figure 5) and at 300 K are 8.87 and 11.4 emu K/mol for **2** and **3**, respectively. These values are in the range expected for four octahedral $S = 1/2$ low-spin Fe^{III} ions, each with an effective moment of ~0.66 emu K/mol,[24a] and either two $S = 3/2$ high-spin Co^{II}, with $\chi T = \sim 3.12$ emu K/mol[24c] for **2**, or two $S = 5/2$ high-spin Mn^{II}, with $\chi T = 4.47$ emu K/mol[24d] for **3**.

Below 100 K $\chi T(T)$ decreases indicating that in each $Co^{II}{}_2Fe^{III}{}_4$ and $Mn^{II}{}_2Fe^{III}{}_4$ cluster at low temperature spins are antiferromagnetically coupled. The linear fit of $\chi^{-1}(T)$ data to Curie−Weiss law in the 50−100 K range yields negative Θ (−3.7 and −3.3 K for **2** and **3**, respectively) in accord with the presence of unpaired spins in the t_{2g} orbital. Below 20 K $\chi T(T)$ for **2** increases indicating a magnetic transition presumably of the similar (canted) origin as in **1**. In contrast, $\chi T(T)$ for **3** decreases rapidly implying that canting does not occur, as expected for the negligible single ion anisotropy observed for high-spin Mn^{II}.[28]

(27) In our symmetric ($\sim D_{2h}$) Fe_4M_2 magnetically coupled clusters single ion anisotropy of each ion is most probably averaged, and therefore, we assumed that the g-factor of the cluster is close to 2 as it was observed, for instance, in the $Mn^{III}-Fe^{III}-Mn^{III}$ $S = 9/2$ cluster with g-factor of 2.03 (Ferbinteanu, M.; Miyasaka, H.; Wernsdorfer, W.; Nakata, K.; Sugiura, K.; Yamashita, M.; Coulon, C.; Clérac, R. *J. Am. Chem. Soc.* **2005**, 127, 3090).

(28) Carlin, R. L. *Magnetochemistry*; Springer-Verlag: Berlin, Heidelberg, Tokyo, 1986; p 148.

Interestingly, upon the annealing of **2** in a vacuum at 300 K $\chi T(T)$ is changed (Figure 3). Below 120 K with decreasing temperature, $\chi T(T)$ reaches a maximum at ~5 K and then decreases; similar to the case for **1**, Θ changes sign to 3.6 K. The change in the ν_{CN} stretching frequencies gives useful information. The spectrum of **2** shows two main peaks at 2157 and 2131 cm^{-1}. The higher frequency is assigned to the stretching vibration of the bridging CN and the lower frequency to the terminal CN, as the terminal CN of $[Fe(Tp)(CN)_3]^-$ is observed at 2129 cm^{-1} as a sharp singlet. Upon annealing, the terminal stretching vibration of **2** disappears and a new peak appears at 2150 cm^{-1} . This significant shift toward higher frequency implies that all the cyanide ligands of annealed sample bridge Fe^{III} and Co^{II} ions. Similar observation of peak shift of CN group has been reported by other group.[29] FTIR and TGA studies indicate that the coordinating water molecules still existed even in annealed sample of **2**. Thus, loss of coordinating MeCN molecules might lead to further polymerization and a change in magnetic coupling from antiferro- to ferromagnetic. But the possibility of change in coordination sphere of Co^{II} from octahedral to tetrahedral by solvent loss cannot be excluded, because χT for tetrahedral Co^{II} is ~5% smaller than that for octahedral Co^{II} as well as tetrahedral Co^{II} has electronic configuration of $e^4t_2{}^3$. The small decrease of $\chi T(T)$ at 300 K from 8.9 to 8.1 emu K/mol is consistent with the hypothesis.

Conclusion

$[\{Fe(Tp)(CN)_3\}_4\{Ni(MeCN)(H_2O)_2\}_2]\cdot 10H_2O\cdot 2MeCN$ (**1**) is a canted antiferromagnet that undergoes a field-induced spin-flop-like transition at ~1 T at 2 K. At 4.45 K **1** undergoes a transition to paramagnetic state of noninteracting $S = 4$ magnetic clusters. On further warming, the relatively weak FM intracluster coupling fails to compete with thermal agitation, and the material behaves as independent octahedral $S = 1/2$ low-spin Fe^{III} and $S = 1$ Ni^{II} ions. In contrast, **2** and **3** demonstrate antiferromagnetic intracluster coupling in accord with unpaired electron orbital symmetry.

Acknowledgment. This work was financially supported by the Ministry of Science and Technology of Korea (NRL program). The continued partial support by the U.S. National Science Foundation U.S.-Korea Grant No. INT-9910383, the U.S. Department of Energy Division of Materials Science (Grant Nos. DE-FG03-93ER45504, DE-FG02-01ER45931, DE-FG02-86ER45271, and DEFG0296ER12198), and DARPA through the ONR (Grant No. N00014-02-1-0593) is gratefully acknowledged.

Supporting Information Available: Complete details of the X-ray diffraction study of complexes **1**−**3** (CIF). This material is available free of charge via the Internet at http://pubs.acs.org.

IC0500356

(29) Chen, X.-Y.; Shi, W.; Xia J.; Cheng, P.; Zhao, B.; Song, H.-B.; Wang, H. G.; Yan, S.-P.; Liao, D.-Z.; Jiang, Z.-H. *Inorg. Chem.* **2005**, *44*, 4263.